Functional Materials 13, No.2 (2006) © 2006 — Institute for Single Crystals

Some characteristics of semiconductor HgCdMnZnTe solid solution crystals

N.Popenko, I.Ivanchenko, I.Brovenko, A.Zhigalov, S.Karelin, I.Gorbatyuk, S.Ostapov*, S.Dremlyuzhenko*, I.Rarenko*, R.Zaplitnyi*, I.Fodchuk*, V.G.Deibuk**

A.Usikov Institute for Radiophysics and Electronics, National Academy of Sciences of Ukraine, 12 Proskura St., 61085 Kharkiv, Ukraine
*Chernivtsi National University, 2 Kotsyubinsky St., 58012 Chernivtsi, Ukraine

Received 25 February, 2005

A novel semiconductor solid solution HgCdMnZnTe containing up to 5 % of manganese and zinc has been studied. Microhardness of these crystals and galvanomagnetic characteristics have been measured out as well as the X-ray structure analysis thereof. The band-gap width, intrinsic charge carrier concentration and mobility have been determined. It is shown that the novel material has more perfect crystal structure as compared to HgCdTe. The obtained data allow announcing this material as an alternative one for manufacturing effective infrared detectors operating in the 3–5 μm and 8–14 μm spectral ranges.

Представлены результаты исследования нового полупроводникового твердого раствора HgCdMnZnTe с содержанием марганца и цинка до 5 %. Проведены исследования механических свойств и гальваномагнитные измерения этих кристаллов, а также проведен их рентгеноструктурный анализ. Определены основные электрофизические параметры, такие как ширина запрещенной зоны, концентрация и подвижность собственных носителей заряда. Показано, что новый материал имеет более совершенную кристаллическую структуру по сравнению с HgCdTe. Полученные данные позволяют сделать вывод о том, что данный материал может рассматриваться как альтернативный при создании эффективных фотоприемников, работающих в спектральных диапазонах 3–5 мкм и 8–14 мкм.

The well-known semiconductor HgCdTe for manufacturing IR detectors operating in a wide spectral range (1–14 μm) has serious shortcomings. In the first place, it is a crystal lattice temporal instability due to a weak binding of mercury atoms in the lattice. This causes in the formation of electrically active mercury vacancies being acceptors resulting in the level redistribution of electrically active current carrier centers [1, 2]. Second, it is a considerable dependence of the bulk material properties and especially of the surface ones on the perfection of HgCdTe crystal structure. The structural macrodefects (unit boundaries, different phase precipitates, etc.) and microdefects (dislocations, local stoichiometry deviations) bring about not only local photosensitivity inhomogeneities of HgCdTe based devices, but also the instability of their parameters [3, 4].

We assume that a new semiconductor HgCdMnZnTe solid solution with low content of manganese and zinc (up to 5 %) can be free of the above-mentioned drawbacks of HgCdTe. The grounds for this are the following arguments. The full or partial replacement of Cd atoms by Mn ones in

HgCdTe solid solution results in an improvement of both the crystal structural perfection (increased unit dimensions, reduced unit disordering, lower density of dislocations) [5] and surface properties [6]. However, it is impossible to obtain the pure uncompensated HgMnTe crystals with less than 10^{15} am^{-3} donor concentration due to the complicacy of manganese purification and its high chemical activity. On the other hand, a partial replacement of Cd atoms by Zn ones improves temporal and thermal stability of HgCdTe crystals, as well as reduces the formation of mercury vacancies and their migration rate to the surface [7]. At the same time, a full replacement of cadmium atoms by zinc ones gives rise to the embrittlement of crystals, apparently due to the considerable crystal lattice intensity [8].

It is known that the crystals of HgCdTe class, including HgCdMnZnTe as well, have segregation coefficient exceeding 1. It means that the content of components along the grown ingot is inhomogeneous. With these remarks in mind the main goal of this paper is the experimental study of structural, mechanical, main band gap and electrophysical parameters of HgCdMnZnTe crystals grown recently to determine the ingot regions, in which the aforementioned parameters coincide with those for HgCdTe crystals as soon as better.

HgCdMnZnTe crystals were grown by the modified zone melting method from the presynthesized homogeneous polycrystalline ingots of 18 mm in diameter and 16 cm in length. To synthesize the solid solutions, we used initial components Cd, Te, Zn, and Hg of a purity of at least 99.9999 mass.% and Mn of a purity 99.998 mass.% purified additionally by double vacuum distillation. Modification of the traditional vertical zone melting method consists in growing of the crystals at the angle to the horizon from 30° to 60° under intensive agitation of the melt by axial rotation. Two sets of $Hg_{1-x-y-z}Cd_xMn_yZn_zTe$ ingots, hereinafter referred to as set-1 and set-2, respectively, were grown at different initial contents of components, namely: for the set-1 of ingots, $x = 0.14$; $y = 0.02$; $z = 0.01$; for the set-2 of ingots, $x = 0.1$; $y = 0.04$; $z = 0.01$. At those ratios of solid solution components the energy gap corresponds to operating frequencies of IR detectors. The samples in the form of plane-parallel wafers were cut out of the ingots perpendicularly to the growth direction and equally spaced with respect to the ingots beginning. For the sake of narrative simplicity, we have tentatively divided all the ingots under study into three equal parts, namely: initial (a), middle (b) and terminal (c), respectively, and five samples were cut out from each of those parts.

The structural perfection of HgCdMnZnTe crystals was investigated by X-ray Berg-Barrett method. The investigations have shown that all HgCdMnZnTe samples have the unitized structure with disorientation angles between the units within 30–400 arc seconds. It is worth noting that with the increasing number of components in semiconductor solid solutions under consideration, the unit dimensions increases from (0.2–0.6) mm for HgCdTe to (0.5–1.5) mm for HgMnCdTe, and to (0.9–4.5) mm for HgCdMnZnTe. Thus, 7-8-fold increase of unit dimensions with respect to HgCdTe ones indicates the improved crystalline structure of the novel five-component solid solution. To obtain an additional evidence for the crystal structure improvement, we have performed the microhardness investigations. According to the results obtained, the crystal microhardness increases with increasing Cd, Mn and Zn content. The study illustrates that the microhardness of crystals cut out of the second set of ingots is also about 8 % higher. Thus, the X-ray and mechanical investigations allow announcing the more perfect crystal structure of HgCdMnZnTe as compared to HgCdTe.

The energy gap of HgCdMnZnTe crystals was determined from the fundamental absorption curves at room temperature, as long as all the grown crystals were optically transparent. The transmission of samples was varied from few per cent to 60 %. The fundamental absorption edge was in the wavelength range 4 to 8 μm, thus corresponding to the energy gap width from 0.15 eV to 0.3 eV.

However, to discuss the conformity between parameters of HgCdMnZnTe and HgCdTe materials, we have to compare their temperature dependences of charge carrier concentrations and mobility. In this connection, we have measured galvanomagnetic characteristics in the temperature range 4.2–300 K using the setup described in [9].

According to the experimental data, the samples from the set-1 of ingots have a lower concentration of manganese, and, hence, a narrower energy gap. Moreover, all the samples cut out of the initial and middle parts have n-type conductivity within the range from room temperature to liquid helium one (Table 1). For the samples cut

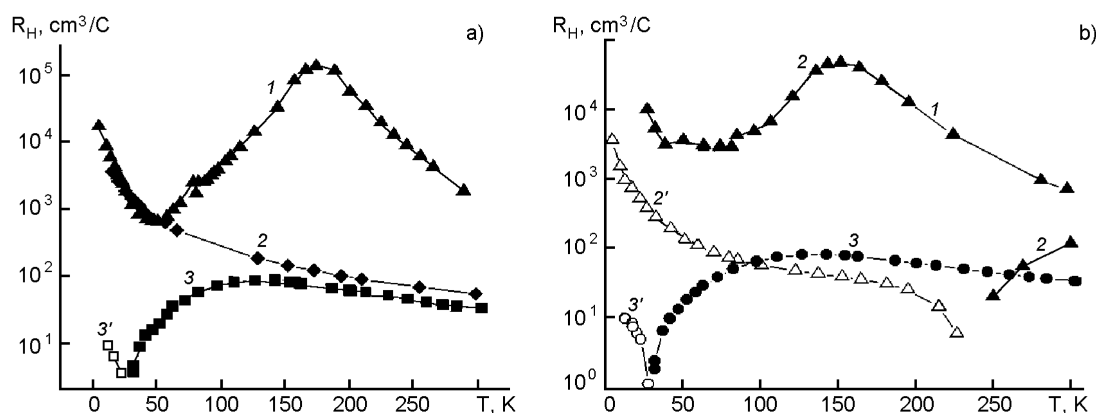

Fig. 1. Hall coefficient for HgCdMnZnTe samples cut out of the first set of ingots (a) and second one (b) vs. temperature. (a): *1* — 1_a; *2* — 1_b; *3,3′* — 1_c; (b): *1* — 2_a; *2,2′* — 2_b; *3,3′* — 2_c (black icons correspond to $R_H < 0$, and white icons correspond to $R_H > 0$).

out of the terminal part of ingots, there is a conversion to *p*-type conductivity at helium temperatures (Fig. 1a; for simplicity sake, we show here and further only one of the curves similar in run).

For the samples 1_a we can observe a peak on the temperature dependences of Hall coefficient. As to the samples 1_c, a similar peak is shifted towards lower temperatures, and its magnitude decreases gradually. For the samples 1_b this dependence demonstrates monotonous rise with the temperature decreasing. At the same time, in samples from terminal part of ingots there is a conversion to *p*-type conductivity at temperatures $T < 50$ K. We note that at room temperature, the conductivity of the samples is changed within limits of 2.4 to 809 $(\Omega\cdot\mathrm{cm})^{-1}$ (Table 1). Moving to the lower temperatures the conductivity decreases and at helium temperatures it is varied within limits of 0.004 to 126 $(\Omega\cdot\mathrm{cm})^{-1}$.

Adverting to the temperature dependences of Hall coefficients for the samples from the set-2 of ingots, we can see that for the samples 2_a (Fig. 1b, curve *1*) this dependence is similar to that for the 1_a samples of the set-1 of ingots (Fig. 1a, curve *1*). However, unlike the samples from the set-1, the samples 2_b demonstrate a change in the Hall coefficient sign at temperatures 200–230 K (Fig. 1b, curve 2), that testifies to a wider energy gap and smaller concentration of intrinsic carriers. The region of this conversion is shifted to lower temperatures for the samples 2-c (Fig. 1b, curve *3*). This behavior is similar to that for the 1_c samples (Fig. 1a, curve *3*). Here, the conductivity of all the samples from the set-2 of ingots is essentially lower as compared to that of the samples from the first set of ingots and its magnitude is found to be within limits of 0.17 to 172 $(\Omega\cdot\mathrm{cm})^{-1}$ at room temperature. For the samples 2_c, the

Table 1. Kinetic characteristics of HgCdMnZnTe samples

Samples	Conductivity type			$n\cdot10^{15}$ cm^{-3}			$\sigma(\Omega\cdot\mathrm{cm})^{-1}$	$\mu\cdot\mathrm{cm}^2/(\mathrm{V\cdot s})$
	4.2	77	300	4.2	77	300	300	77
$HMg_{1-x-y-z}Cd_{0.14x}Mn_yZn_zTe$ (set-1: x = 0.14, y = 0.02, z = 0.01)								
(1_a)	*n*	*n*	*n*	0.36	0.25	3.3	2.46	43.6
(1_b)	*n*	*n*	*n*	1.7	12.8	115	745	2.9105
(1_c)	*p*	*n*	*n*	867	70.8	225	809	4.3
$Hg_{1-x-y-z}Cd_xMn_yZn_zTe$ (set-2: x = 0.1, y = 0.04, z = 0.01)								
(2_a)	*n*	*n*	*n*	0.62	2.2	8.9	3.88	44.3
(2_b)	*p*	*p*	*n*	1.1	89.3	52.3	2.95	203.8
(2_c)	*p*	*n*	*n*	694	147	212	172	966

conductivity is ten times lower when passing to helium temperatures.

Thus, the comparison of results concerning the galvanomagnetic measurements for the samples cut out of the same regions of ingots from two sets of ones with different initial manganese content (2 % and 4 %, respectively) shows the greatest differences in their characteristics. Moreover, the increase in initial manganese content results in a change in the Hall coefficient sign.

Basing on the results of galvanomagnetic measurements, the charge carrier concentration and mobility were calculated (Table 1). It has been found that the concentration in all the samples from the set-1 of ingots at room temperature is varied less than by 2 orders. At nitrogen temperatures, the carrier concentration is within limits of $5.2\cdot10^{14}$ cm^{-3} to $7\cdot10^{16}$ cm^{-3}, and the further temperature decreasing results in subsequent change of concentrations within limits of $3\cdot10^{14}$ cm^{-3} to $8.67\cdot10^{17}$ cm^{-3}. Unlike the samples cut out of the initial and middle parts of ingots, the samples cut out of the terminal part demonstrate a concentration rise at helium temperatures that should be attributed to a small energy gap width and very high carrier concentration.

The set-2 of ingots, just as the set-1, includes n-type samples at room temperature (Table 1). However, we can observe a change in the Hall coefficient sign for the samples cut out of the middle and terminal parts of ingots with the temperature decreasing.

In order to determine the dominate scattering mechanisms in both sets of ingots, the temperature dependencies of charge carrier mobility are required. It was found that the charge carrier mobility for most of samples from the set-1 of ingots decreases at temperatures below 150–200 K due to the charge carrier scattering on polar optical phonons. A situation like that is typical for materials similar to HgCdTe. At nitrogen temperatures, the charge carrier mobility in the samples from initial part of the ingots drops, that could be explained by charge carrier scattering on ionized impurities (Table 1). At lower temperatures, the carrier freeze-out calls forth even more drastic mobility drop. The charge carrier mobility is in the range of 10 to 10000 cm^2/(V·s) at helium temperatures and reaches ~$5\cdot10^4$ cm^2/(V·s) within the temperature range of 150 K to 200 K. Here, the charge carrier mobility in samples cut out of the middle par t of ingots is very

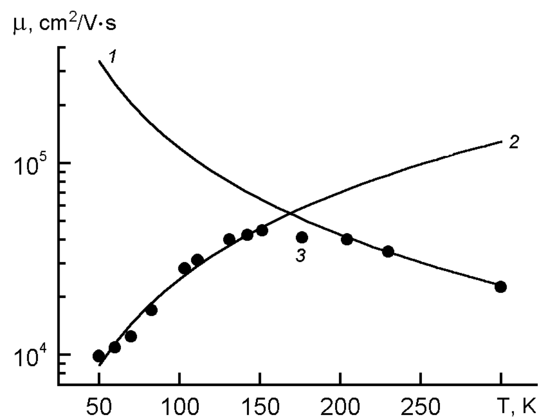

Fig. 2. Experimental and theoretical dependences of charge carrier mobility for the samples 1_b vs. temperature. *1* – optics phonons; *2* – ionized impurities; *3* – experiment.

high ($5–8\cdot10^5$ cm^2/(V·s), which is attributable, in our opinion, to a narrow energy gap (less than 0.22 eV at room temperature) and relatively low impurity content. This results in the preferable phonon charge carrier scattering.

As long as the samples from the set-2 of ingots have a higher manganese concentration, they also have a wider energy gap, which is responsible for the observed conductivity type inversion. The rest of samples demonstrate an impurity scattering only up to room temperature due to the large energy gap and considerable impurity concentration. In the samples from the set-2 of ingots, we cannot observe such high mobility similar to the set-1: the mobility does not exceed $1\cdot10^4$ cm^2/(V·s).

It is worth noting that for some samples under investigation the temperature dependence of charge carrier mobility allows us to estimate the concentration of donors N_D and acceptors N_A. The first one can be simulated from the temperature dependence under assumption of scattering on the polar optical phonons and ionized impurities. The comparison of experimental data for the samples 1_b with calculated ones for the two scattering mechanisms mentioned above allows us to determine the temperature region of their changing (Fig. 2). As it is evident from the Figure, the charge carrier mobility in this sample at temperatures $T > 180$ K is completely defined by scattering on polar optical phonons, while at lower temperatures, on ionized impurities. Such mobility behavior is also typical of some samples from both sets of ingots. To calculate the charge carrier mobility at their scattering

Table 2. Impurity concentration in HgCdMnZnTe samples

No.	Sample	Donor concentration N_D, cm^{-3}	Acceptor concentration N_A, cm^{-3}
1.	I_2.2	$5 \cdot 10^{16}$	$1.3 \cdot 10^{15}$
2.	I_2.3	$3 \cdot 10^{15}$	$7 \cdot 10^{15}$
3.	I_2.4	$3 \cdot 10^{15}$	$1 \cdot 10^{16}$
4.	I_3.3	$6.2 \cdot 10^{15}$	$7 \cdot 10^{16}$
5.	II_3.1	$1.2 \cdot 10^{16}$	$5 \cdot 10^{17}$
6.	II_3.2	$4.8 \cdot 10^{16}$	$2 \cdot 10^{17}$

on ionized impurities, we used the Brooks-Herring formula [10]. The donor and acceptor concentrations were determined for the case when we observe the best coincidence of theoretical curves with experimental ones. Here, the impurity concentration was varied from $1.3 \cdot 10^{15}$ cm^{-3} to $5 \cdot 10^{17}$ cm^{-3}. It suggests that the samples could be both the degenerate semiconductors and non-degenerate ones. At room temperature, there is an intrinsic conduction type if the impurity concentration is low, at least lower than intrinsic concentration, or the extrinsic conduction type at a high impurity concentration. Using the points of changing the Hall coefficient sign, we estimated the value of electron-hole mobility ratio, which turned out to be about 117. This value is near the established one for given class of materials (100) and testifies the properties similarity of HgCdMnZnTe and HgCdTe crystals.

Finally, we have carried out the calculations of intrinsic carrier concentration as described in [11]. The calculation results for 1_a and 1_b samples are in good agreement with the experiment in the intrinsic region. In our opinion, of a special interest are the samples 1_b with $x = 0.140$, $y = 0.014$, $z = 0.010$ (Fig. 3), since their intrinsic region extends up to 100 K, indicating a low content of defects and, respectively, a high quality of HgCdMnZnTe crystals. For the comparison, Fig. 3 shows the temperature dependences of intrinsic carrier concentration for $Hg_{0.8}Cd_{0.2}Te$ (curve A) and $Hg_{0.7}Cd_{0.3}Te$ (curve B) samples, calculated using the empirical formula for intrinsic carrier concentration in HgCdTe [12]:

$$n_i(x,T) = (8.46 - 2.29x + 0.00342T) \times \times 10^{14} T^{3/2} E_g^{3/4} \exp(-E_g/2k_0T). \quad (1)$$

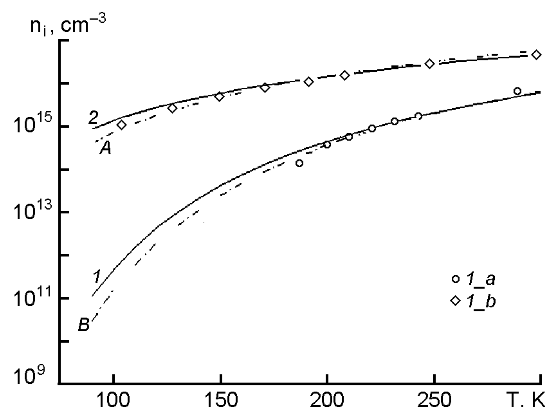

Fig. 3. Intrinsic carriers' concentration vs. temperature in HgCdMnZnTe samples of various compositions. Points are the experimental data, curves are the calculated ones obtained as described in [11]: *1* — $x = 0.190$; $y = 0.025$; $z = 0.012$; *2* — $x = 0.140$; $y = 0.014$; $z = 0.010$. The dotted curve A corresponds to $Hg_{0.8}Cd_{0.2}Te$; the dotted curve B corresponds to $Hg_{0.7}Cd_{0.3}Te$ in accordance with formula (1).

It is seen that the samples 1_b are similar to $Hg_{0.8}Cd_{0.2}Te$ ones in the intrinsic carrier concentration, though they are similar to $Hg_{0.817}Cd_{0.183}Te$ in the energy gap. At the same time, the samples 1_a are similar to $Hg_{0.7}Cd_{0.3}Te$ in the concentration and to $Hg_{0.72}Cd_{0.28}Te$ in the energy gap. Thus, the intrinsic carrier concentration in HgCdMnZnTe is somewhat less than in HgCdTe for the equal energy gap.

Thus, the novel HgCdMnZnTe solid solution has been proposed and its structural, mechanical and galvanomagnetic characteristics have been investigated. It was found that the samples cut out from the middle part of the ingot with an initial content manganese $y = 0.02$ are the optimal ones from their employment for IR receivers point of view. It is worth noting that the concentrations of intrinsic carriers, donors and acceptors are similar to those of HgCdTe crystals, and the charge carrier's mobility reaches the record values about $8 \cdot 10^5$ cm^2/(V·s). Moreover, unlike HgCdTe, they possess a more perfect crystal structure and a higher stability of crystal lattice, which is testified by unit dimensions and microhardness increasing. Everything mentioned above allows announcing that the new five-component solid solution can be considered as an alternative material for IR detectors operating in 3 to 5 μm and 8 to 14 μm spectral ranges.

References

1. G.Nimtz, B.Schlicht, R.Dornhaus, *Appl.Phys. Lett.*, **34**, 490 (1979).
2. H.R.Vydynath, *J.Electrochem.Soc.*, **2609**, (1981).
3. I.S.Virt, N.N.Grigor'ev, A.V.Lyubchenko et al., *Poverkhnost*, No.4, 60 (1988).
4. I.I.Izhnin, *Proc. of SPIE*, **3890**, 519 (1999).
5. O.A.Bodnaruk, I.N.Gorbatyuk, V.I.Kalenik et al., *Neorg.Mater.*, **28**, 335 (1992).
6. O.G.Lanskaya, E.P.Lilenko, A.V.Voitsekhovskii, V.I.Kalenik, *Proc. of SPIE*, **3182**, 111 (1996).
7. R.Granger, A.Lasbley, S.Rolland et al., *Cryst. Growth*, **86**, 682 (1990).
8. I.Rarenko, E.Rybak, Y.Stetsko, Z.Zakharuk, in: E-MRS 1995 Spring Meeting, v.D-III, Stemsbony (1995), p.409.
9. A.Zhigalov, S.Karelin, in: Visnyk of L'viv University (Ukraine), Issue 36 (2003), p.199.
10. W.Scott, E.Stelzer, J.Hager, *J.Appl.Phys.*, **47**, 1408 (1976).
11. I.N.Gorbatiuk, A.V.Markov, S.E.Ostapov et al., *Semiconductors*, **38**, 1369 (2003).
12. J.R.Lowney, D.G.Seiler, C.L.Littler, I.T.Yoon, *J.Appl.Phys.*, **71**, 1253 (1992).

Деякі характеристики напівпровідникового твердого розчину кристалів HgCdMnZnTe

Н.Попенко, І.Іванченко, І.Бровенко, Ф.Жигалов, С.Карелін, І.Горбатюк, С.Остапов, С.Дремлюженко, І.Раренко, Р.Заплітний, І.Фодчук, В.Дейбук

Представлено результати дослідження нового твердого розчину HgCdMnZnTe з вмістом марганцю та цинку до 5 %. Проведені дослідження механічних властивостей цих кристалів та гальваномагнітні вимірювання, а також зроблений їх рентгеноструктурний аналіз. Визначено ширину забороненої зони, концентрацію та рухливість власних носіїв струму. Показано, що новий матеріал має більш досконалу кристалічну структуру у порівнянні з HgCdTe. Отримані дані дозволяють зробити висновок про те, що даний матеріал може бути розглянутий як альтернативний при створенні ефективних фотоприймачів, що працюють у 3–5 мкм та 8–14 мкм спектральних діапазонах.